EUROPEAN JOURNAL OF MATERIALS SCIENCE AND ENGINEERING
Volume 9, Issue 3, 2024: 231-242 | www.ejmse.ro | ISSN: 2537-4338

DOI: 10.36868/ejmse.2024.09.03.231

# INNOVATIVE EXPERIMENTAL TESTING PROGRAM OF DIRECT SHEAR TEST IN SOIL MECHANICS

Zakaria OWUSU-YEBOAH[1], Mircea ANICULAESI[1],
Andreea Vasilica DASCALU[1], Iancu Bogdan TEODORU[1], Irina LUNGU[1]

[1]Faculty of Civil Engineering and Building Services, Gheorghe Asachi Technical University of Iasi, 67 Prof. D. Mangeron Blvd, RO-700050 Iasi, Romania.

**Abstract**

*The research work aims at analyzing for the first time the data set obtained on cohesive soil samples following the publication of the Romanian Invention Patent RO 134239. The standard test method for the direct shear test provides the shear strength parameter – internal friction angle in consolidated drained condition - of either undisturbed or remolded soil samples forcing the shear plane at the midsection of the sample in the horizontal direction. The samples are provided in parallelepipedal shape (6 cm x 6 cm x 2 cm) and the displacement rate in horizontal direction is 0.1 mm/min. The new equipment patented in Romania changes the direction of shearing, from horizontal to vertical, and the soil samples are of cubic shape (6 cm x 6 cm x 6 cm). The experimental program involves testing both the parallelepipedal and cubic samples using the same motorized mechanism, with simultaneous readings from their respective micro-comparators. The UU test is performed without allowing consolidation and shearing at 1.0 mm/min. For the CD test, samples are consolidated under vertical loads for 24 hours before shearing at 0.1 mm/min. The shear stresses for cubic samples were higher than those for parallelepipedal samples, with residual stresses reflecting this trend. For cubic samples, both the peak and residual shear stresses trend lines indicated higher cohesion (c) and lower internal friction angle (ϕ) for UU tests and CD tests in contrast to parallelepipedal samples in both testing conditions. The innovative testing program allows for variability in shear strength parameters along the soil failure surface in both natural and compacted soil structures. This differentiation divides the soil condition into drained and undrained states at the initiation, emergence points, and the point of maximum depth along the failure surface. This approach is significant for accurately assessing soil shear resistance and potential failure mechanisms. The study's findings suggest a nuanced approach to parameter selection for slope stability analysis, ensuring accurate representation of both cohesion and internal friction in stability models.*

**Keywords:** *direct shear test, shear strength parameters, soil mechanics, soil cohesion, internal friction angle.*

## Introduction

### *Investigating the Importance of Shear Strength Application in Soil Mechanics*

Shear strength is an important property of cohesive soils that defines the ability of soils to resist the maximum shear stress along their internal surfaces before failure. The fundamental parameters governing soil shear strength – cohesion ($c$) and internal friction angle ($\varphi$) – have long been central to geotechnical engineering, critical for assessing soil stability under different site conditions (1). The determination of shear strength is fundamental to foundation design, slope stability analysis, design of dams and embankments, retaining walls, tunnels and assessing

*Corresponding author: zakaria.owusu-yeboah@student.tuiasi.ro

landslide risk. The shear strength parameters are used to design foundations safely to prevent structural failure and also help determine the critical slip surface and factor of safety to ensure the stability of slopes (2). In retaining wall construction, shear strength is essential for calculating lateral earth pressures and the assessment of shear strength are crucial for the determination of soils ability to withstand forces due to water pressure, self-weight and seismic activity in embankment, dam and tunnel design (3).

Accurate shear strength knowledge is critical for the design of geotechnical structures to ensure resilience to estimated loads and environmental conditions. Understanding shear strength enables engineers to identify and mitigate potential soil structure failures in order to prevent disasters such as landslides or foundation collapses (4; 5). The application of shear strength principles results in the efficient utilization of materials and cost reduction while at the same time adhering to industry safety standards. These applications play an important role in environmental sustainability by preventing soil structure failures (6). Innovations in construction methods and materials are supported by shear strength knowledge and application soils which enhance soil-structure performance (7). Shear strength data is essential in risk assessment models for evaluating geotechnical failure probabilities and impacts, facilitating strategic decision-making. The application of shear strength principles underlines sustainable development by recommending long-lasting geotechnical solutions with minimal maintenance. The application of shear strength in soil mechanics is a multifaceted field that encompasses innovative research to properly understand soil behaviour under different testing techniques and analytical modelling.

***Laboratory Techniques for Determining Shear Strength of Soil***

Historically, the measurement of shear strength in soils began with simple shear tests developed in the early 20th century which allowed for more accurate and practical assessment of soil shear strength under controlled conditions (1). The earliest and simplest method developed was the Direct Shear Test. This method is straightforward and widely used, but it has some drawbacks which resulted in the development of other methods to overcome them. The Triaxial compression test was developed to overcome the limitations of the direct shear test. The triaxial test can measure both drained and undrained shear strength parameters and can simulate various stress paths encountered in the field (8; 9). This test is complex and time-consuming compared to the direct shear test. The Unconfined Compression Test is another technique used primarily for cohesive soils. This test is quick and easy to perform but is only suitable for soils that can stand without lateral support, limiting its applicability to cohesive soils and making it unsuitable for loose or granular soils (10). As the need for more precise and varied testing conditions grew, the Ring Shear Test was introduced. This test allows for the continuous rotation of the soil specimen, enabling the study of large shear deformations and the residual shear strength of soils (11). This test is less common and more specialized than the direct shear test or even triaxial tests.

Modern advancements have also led to the development of the Centrifuge Test, which uses a centrifuge to simulate gravitational forces on small-scale soil models. This technique is particularly useful for studying complex geotechnical problems, such as the behavior of earth structures under different stress conditions. The centrifuge test offers valuable insights into soil behavior under realistic stress conditions, but it requires sophisticated equipment and expertise, limiting its widespread use (12). Another recent development is the Bender Element Test which is used to measure the small-strain shear modulus of soils. Although it is highly effective for determining the dynamic properties of soils, it is typically used in combination with other tests to provide a comprehensive understanding of soil behavior (13). Despite all these advanced methods of determining the shear strength of soils, the direct shear test is still predominant in soil mechanics.

***The Direct Shear Testing Program/Devices***

The concept of the direct shear test device dates back to 1846 when French engineer Alexandre Collin developed a direct shear testing apparatus for slope stability studies in cohesive soils. In 1932, Arthur Casagrande refined the design for a new shear box during his research at Harvard University (14). The direct shear test is a relatively simple soil mechanics test conducted on cohesive or non-cohesive soil samples which are either undisturbed or remolded. The current direct shear devices apply predetermined vertical loads ($\sigma_i$) to the sample and shearing is forced along the midsection with the bottom half of the shear box held in place while the shear machine applies a controlled force to move the upper half in the horizontal direction (15). The samples are provided in parallelepipedal shape (6 cm x 6 cm x 2 cm) and the displacement rate in horizontal direction is 0.1 mm/min for consolidated drain conditions. This test is cost-effective, easy to perform and also the parameters ($\varphi;\ c$) obtained are used to estimate the critical initial pressure and or the bearing capacity of foundation soils.

The model for estimating the bearing capacity of the foundation soil usually considers that the failure surface occurs along a cylindrical surface in the form of a circle or logarithmic spiral as shown in Fig. 1 (16; 17). In the Fig., the failure surface experiences the normal stress in different planes. At the initiation and emergence points (a) and (c) the normal stress is imposed at either vertical ($\sigma_1$) or horizontal ($\sigma_3$) to the surface of shear failure. In contrast, at the deepest level (b), the normal stress ($\sigma_1$) is horizontally tangential to the surface of shear failure. Consequently, the shear resistance parameters internal friction angle and cohesion denoted as ($\varphi_1;\ c_1$) vary at different points ($i$) along the failure surfaces. This variability is predominant at the initiation and emergence points of the failure with parameters ($\varphi_2;\ c_2$) where the failure occurs more closer in the vertical plane than in the horizontal and the point of maximum depth ($\varphi_1;\ c_1$) where failure occurs in the horizontal plane. However, in the current direct shear testing, which is modelled for failure at the deepest point (b), the parameters obtained from this single point ($\varphi_1;\ c_1$) is assumed for the entire failure surface for modelling and design. Nevertheless, this variability is significant in accurately assessing the shear resistance of soils and their potential failure mechanisms.

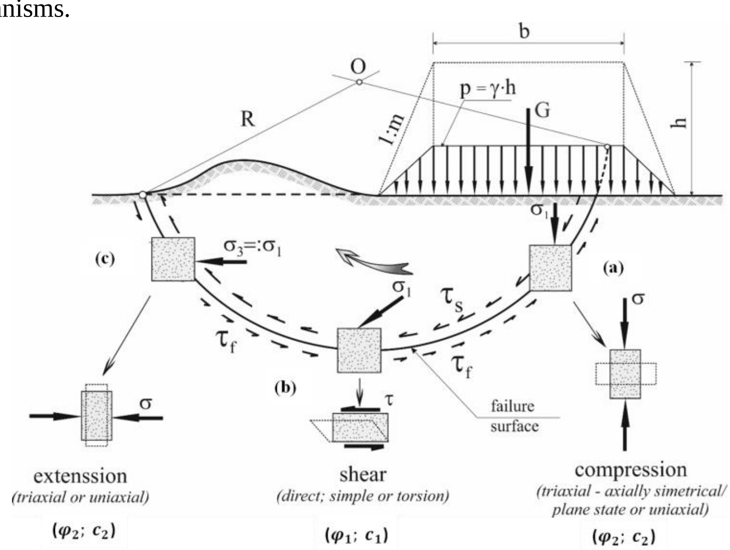


**Fig. 1.** Types of soil stresses along a failure surface and appropriate tests for determining shear strength (18)

This paper aims to analyse, for the first time, a dataset obtained from cohesive soil samples following the publication of the Romanian Invention Patent RO 134239 (19). This patent alters the direction of shear testing from horizontal to vertical using cubic samples with (6 cm x 6 cm x 6 cm) instead of the parallelepiped-shaped sample (6 cm x 6 cm x 2 cm) as depicted in Fig. 2.

The paper explores the variability of the shear strength parameters by comparing the innovative shear testing program with the standard direct shear tests in different soil conditions. The research also evaluates the implications of the findings for the design and stability analysis of man-made and natural slopes.

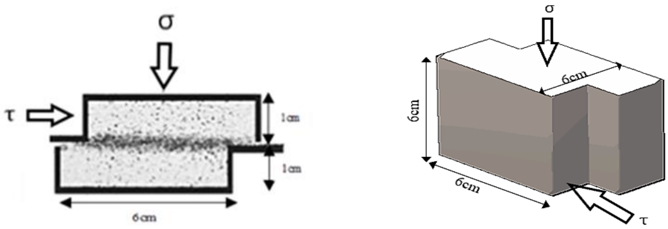


a) b)
b)

**Fig. 2.** Specimens sheared on the imposed forced plane: a) parallelepipedal specimen (6 x 6 x 2 cm) and horizontal shear plane; b) cubic specimen (6 x 6 x 6 cm) and vertical shear plane.

*The New Shearing Machine*

The new shearing device, designed to impose direct shearing on a vertical plane using cubic soil samples (6 cm x 6 cm x 6 cm), comprises five main sub-assemblies, as illustrated in Fig. 3.

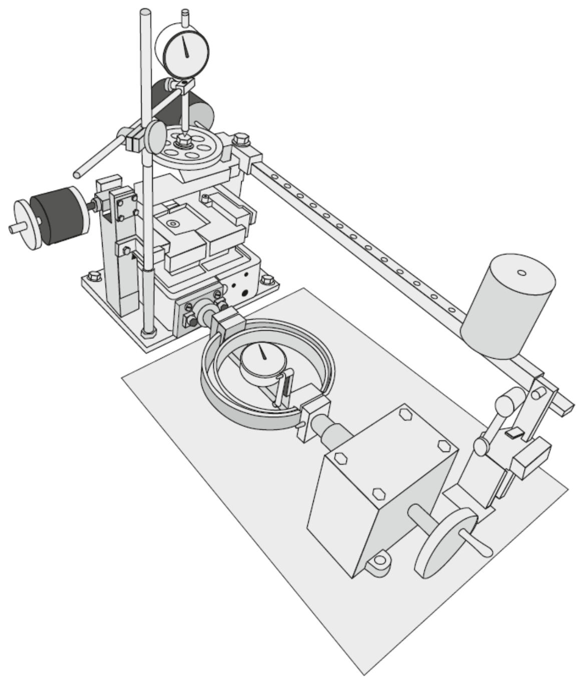

**Fig. 3.** General layout of the new vertically imposed plane shear apparatus for cubic-shaped specimens

This new shear machine is similar in overall layout and operation with the standard direct shear machine but with some exceptions which are illustrated within the Figs. below. The first sub-assembly consists of the levers group which comprises of the weights, counterweights, and a vertical screw to apply the axial load/force on the specimen similar to the standard machine. The second sub-assembly is the shear force application and measurement group which is made up of the marked screw reducer, a drive wheel, a special bushing coupling, the dynamometric rings and a micro-comparator for measuring shear deformation. Sub-assembly three is the shear box group specially designed for shearing in the vertical plane and consists of box itself uniquely in two-cut halves, the shearing semi boxes with cutting knives and the related supporting equipment as depicted in

Fig. 4.

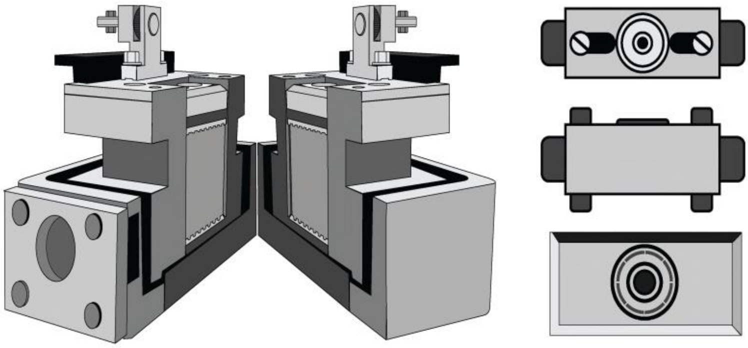

**Fig. 4.** The third sub-assembly - Shear box group showing the uniquely two-cut halves, cutting semi-boxes with associated equipment and the pistons

The fourth sub-assembly is the box support group which is made of the base plate, the tracks for shear boxes, support columns, guides for cutting knives, micro-comparator for measuring consolidation and the support for the micro-comparator as illustrated in Fig. 5.

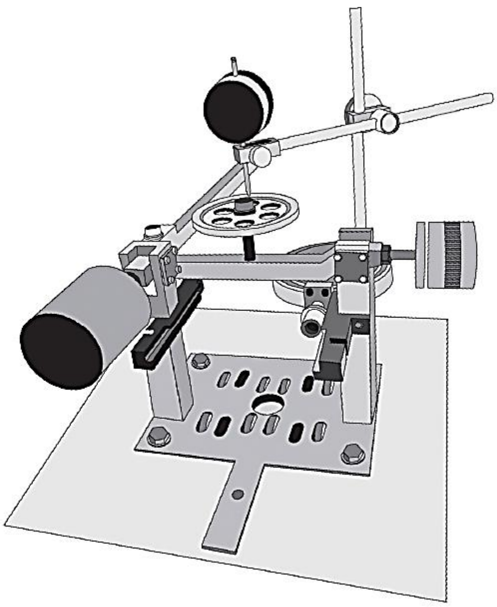

**Fig. 5.** The fourth sub-assembly - Box support group with base plate and tracks for shear boxes

The fifth sub-assembly is the metal plate that supports all the other sub-assemblies just like in the standard shear machine, including the shear box, mounted on a metal frame. It also includes the shearing motor and the electric motor with the gearbox to drive the reducer, thus regulating the shearing speed.

## Materials and Methods

### *Materials and Sample Collection*

This study makes use of baseline soil which were collected from Copou in Iași County of Romania from a depth of 1 to 2 meters to capture the variability in soil properties at different strata. The samples were extracted in the form of monoliths and bagged samples and immediately sealed in airtight containers to preserve their natural moisture content and transported to the laboratory for further testing. The physical properties of the soil were investigated through a series of laboratory tests. The grain size distribution was analysed using the hydrometer analysis following the standard protocols (STAS 1913/5-85). The distribution indicates a predominance of silt with a fraction of 63.53 % with 26.94 % of clay and 9.53 % of sand. The classification suggest that the soil is primarily silty clay (si.Cl). The Atterberg limits indicate a liquid limit (LL) of 36.49 %, a plastic limit (PL) of 24.09 % and a plasticity index of 12.40 %. The soil has medium plasticity consistent with its silty clay classification. The unit weight ($\gamma_{bulk}$) was measured at 16.84k N/m$^3$ and the dry density ($\rho_d$) was 1.73 g/cm$^3$. The soil was slightly moist with a degree of saturation ($S_r$) of 0.36 and void ratio of 0.64. The soil has a porosity of 38.9 % and compaction revealed it having an optimum moisture content (OMC) of 14.93 %.

*Sample Preparation*

The soil specimens were prepared by oven-drying at a temperature of 105°C, and subsequently milled and sieved. Using the obtained dry density and the optimum moisture content, the samples were mixed in air tight plastic bags to prevent moisture lost (Fig. 6a). The samples were then molded using static compaction (packing) technique with the TriTech 50 kN compressor (Fig. 6b) to mold the samples in stainless steel molds. Two different sample sizes were used: cubic with 6 cm x 6 cm x 6 cm and parallelepipedal with 6 cm x 6 cm x 2 cm. For the cubic sample (Fig. 6d), the soil was placed and compacted in three layers each at a rate of 1.25 mm/min to the desired height of 6 cm. The parallelepipedal sample (Fig. 6c) was compacted uniformly at the rate of 1.25 mm/min to the required height of 2 cm. Once compacted, the samples were carefully extruded from the mold to avoid any disturbance. The compacted samples were then trimmed to ensure precise dimensions. A total of six samples of each size (cubic and parallelepipedal) were prepared for Unconsolidated Undrained (UU) and Consolidated Undrained (CU) tests. Each sample was tested to failure in the shear box apparatus, and the resulting shear strength parameters were recorded for further analysis.

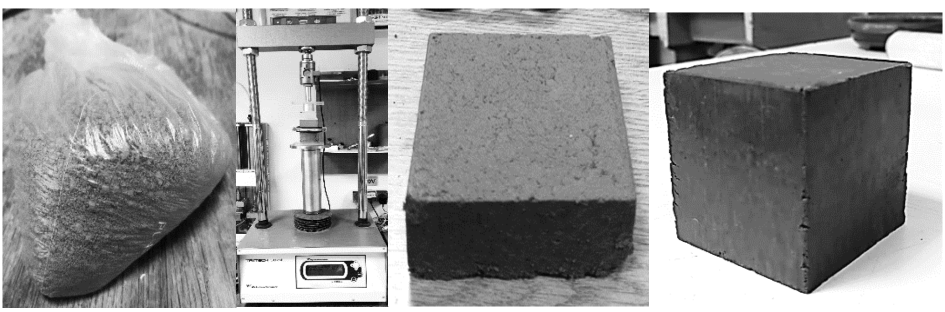

a) b) c) d)

**Fig. 6.** (a) Soil mixture in plastic bags (b) Tritech 50kN compressor (c) parallelepipedal sample (6 cm x 6 cm x 2 cm) (d) cubic sample (6 cm x 6 cm x 6 cm)

*Testing Procedure*

The test procedure began with the assembly of the new shear box for the vertical shearing. First, the two half-boxes are joined face-to-face, with the shearing semi boxes with cutting knives inserted and the assembly secured using two yokes. The two porous stones and two perforated ribbed plates (dimensions 6 x 2 cm) are then placed inside. The inner walls are lubricated and the cubic sample is inserted. Two porous stones and perforated ribbed plates are placed on top as well followed by the two pistons (6 x 3 x 1.5 cm) with a bearing each at their centers. Two bolts of the device, driven by two sliding cylindrical bolts separated by a central spring, are inserted into the central holes of the bearings. This setup ensures the constant maintenance of vertical loads (*N/2* on each piston) throughout the shearing process on the vertical plane of the specimen. The fully assembled and equipped box is then placed on the tracks, with the guide ears of the knives on the guide. A screw for vertical loading is placed in the central hole of the bearing, and the levers are balanced by placing the weights corresponding to vertical loads *N* and vertical stresses $\sigma_1 = N/A$, with A = 60 x 60 $mm^2$. After inserting the box on the tracks and guides, the central pivot is placed in its slot. The device for forward-backward actuation of the half-boxes and the knives is then connected through two arms, with one end fixed to the back of the boxes and the other to the device. Finally, the shear box is coupled through the left half-box, via the bushing, to the elements of sub-assembly two, which applies the shear/cutting force (τ).

The standard shear box is similarly assembled for the horizontal shearing. Initially, the lower half of the shear box is placed in position on the base plate, ensuring it is securely attached to prevent any movement during the test. A porous stone and a perforated ribbed plates (both of dimension 6 x 6 cm) are placed at the bottom and top of the parallelepipedal sample. The sample is then carefully placed into the lower half of the shear box. The loading cap is placed on the top once the sample is secured in the shear box. The assembled box is placed on the tracks with the help of the guide ears. A screw for vertical loading is screwed into the hole on the loading cap for constant application of vertical load with the levers balanced by the application of the vertical loads *N* and vertical stresses $\sigma_1 = N/A$. The shear box is then attached to the horizontal drive mechanism.

The two shear boxes are then subjected to the shearing from the same controlled motorised mechanism and readings are taken simultaneously from their respective micro-comparators. For the UU test, there was not allowed consolidation and the shearing was done at a rate of 1.0mm/min. With the CD test, the samples were placed in with the vertical loads application and allowed to consolidate for 24 hours and afterwards sheared at a rate of 0.1 mm/min. Readings were taken from the consolidation micro-comparators for each of the boxes. After shearing three cubic and three parallelepipedal samples for each test condition (i.e. UU and CD) at different vertical stresses ($\sigma_1^1 = 100\ kPa, \sigma_1^2 = 200\ kPa\ and\ \sigma_1^3 = 300\ kPa$) with the resulting values ($\tau_1^1 < \tau_1^2 < \tau_1^3$), a Coulomb's failure envelope could be drawn to determine the parameters ($\varphi_1;\ c_1$) and ($\varphi_2;\ c_2$).

## Results Analysis

### *Coulomb Failure Envelope Analysis*

The tests conducted on both cubic and parallelepipedal soil samples under both Unconsolidated Undrained (UU) and Consolidated Drained (CD) conditions revealed distinct shear stress behaviors under varying normal stresses. The shear stresses for the cubic samples were observed to be relatively higher than that of the parallelepipedal samples. Their residual shear stresses were relatively consistent with this observation. The data from the tests were plotted on shear stress versus normal stress graphs to derive the Coulomb failure envelopes.

For the cubic samples, the linear trend line fitted in Fig. 7 (a and b) for the peak shear stress points yielded a cohesion (c) value of 175.31 kPa and an internal friction angle ($\phi$) of 20$^o$ for the UU tests, and cohesion (c) of 189.95 kPa and internal friction angle ($\phi$) of 18.4$^o$ for the CD tests. The residual shear stresses yielded c = 149.96 kPa and $\phi$ = 20.5$^o$ for the UU tests and c = 160.67

kPa and $\phi$ = 17.8º for the CD tests. These differences highlight the effect of drainage conditions on the soil's shear strength parameters.

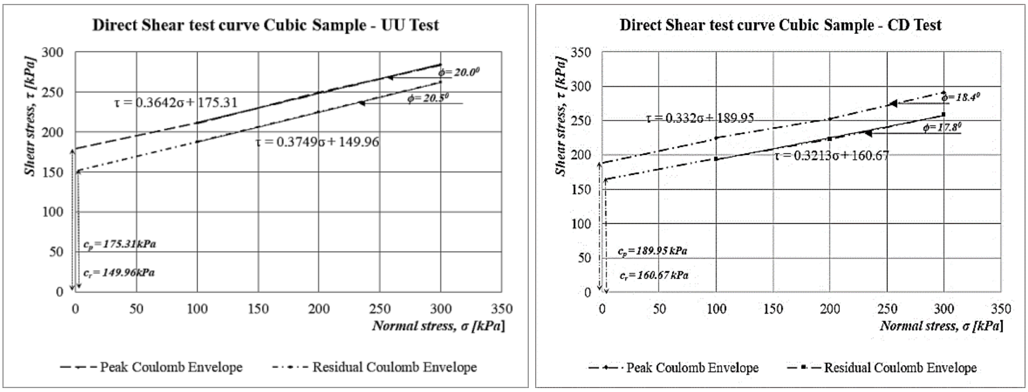


a) b)

**Fig. 7**. Mohr Coulomb failure envelope for the Cubic Samples:
a) Unconsolidated Undrained (UU) condition; b) Consolidated Drained (CD) condition

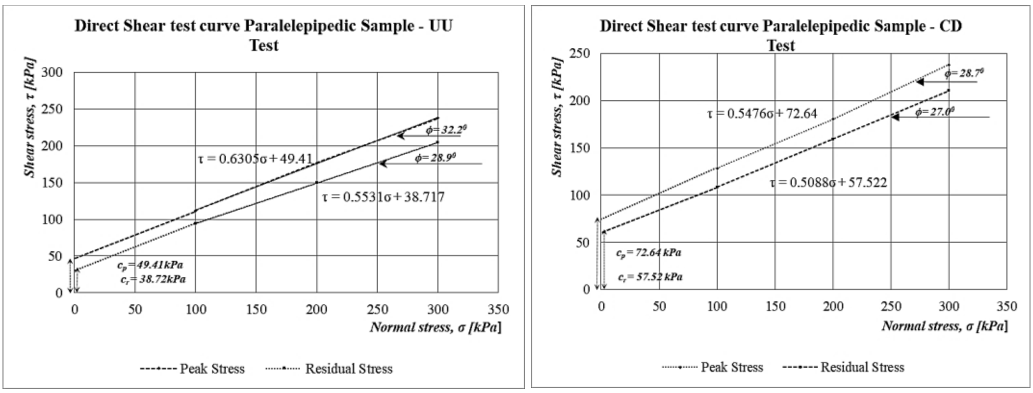


a) b)

**Fig. 8.** Mohr Coulomb failure envelope for the parallelepipedal samples:
a) Unconsolidated Undrained (UU) condition (b) Consolidated Drained (CD) condition

In contrast, the linear trend line fitted in Fig. 8 (a and b) to the peak shear stress points for the parallelepipedal samples yielded a cohesion (c) value of 49.41 kPa and an internal friction angle ($\phi$) of 32.2º for the UU tests, and cohesion (c) of 72.64 kPa and internal friction angle ($\phi$) of 28.7º for the CD tests. The residual shear stresses yielded c = 38.72 kPa and $\phi$ = 28.9º for the UU tests and c = 57.52 kPa and $\phi$ = 27º for the CD tests.

The summary of all the results from the Mohr Coulomb envelopes is in Table 1.

**Table 1.** Tabulated Results of Internal friction angle and cohesion for peak and residual shear strength of soil

| | **Unconsolidated Undrained (UU) Test** | | | | **Consolidated Drained (CD) Test** | | | |
|---|---|---|---|---|---|---|---|---|
| | Cubic Sample (6cm x 6cm x 6cm) | | Parallelepipedal sample (6cm x 6cm x 2cm) | | Cubic Sample (6cm x 6cm x 6cm) | | Parallelepipedal sample (6cm x 6cm x 2cm) | |
| | Internal friction angle (ϕ) | Cohesion (c) [kPa] | Internal friction angle (ϕ) | Cohesion (c) [kPa] | Internal friction angle (ϕ) | Cohesion (c) [kPa] | Internal friction angle (ϕ) | Cohesion (c) [kPa] |

| | | | | | | | | |
|---|---|---|---|---|---|---|---|---|
| | [deg ($^0$)] | | [deg ($^0$)] | | [deg ($^0$)] | | [deg ($^0$)] | |
| **Peak** | 20.0 | 175.31 | 32.2 | 49.41 | 18.4 | 189.95 | 28.7 | 72.64 |
| **Residual** | 20.5 | 149.96 | 28.9 | 38.72 | 17.8 | 160.67 | 27.0 | 57.52 |

***Shear Stress vs. Displacement Curves Analysis***

The shear stress versus displacement curves for both the cubic and parallelepipedal samples are illustrated in Fig. 9 and

Fig. **10** for UU and CD conditions to indicate the peak and residual behavior of the soil samples. For all the test samples in the case of both sample sizes, the peak shear stresses were achieved at displacements of approximately 6 mm, after which a noticeable drop to residual values was observed, stabilizing around 12 mm. The cubic samples had relatively closer shear stress intervals for the application of the three different normal stresses compared to the parallelepipedal samples. The closer values of shear stress intervals for the cubic samples could indicate the minimal effect of vertical normal stresses in the vertical shear failure of sample. The higher values of the residual stresses for the for the CD tests indicate that the soil achieves its maximum strength and subsequently exhibit great strength during strain-softening when drainage is allowed.

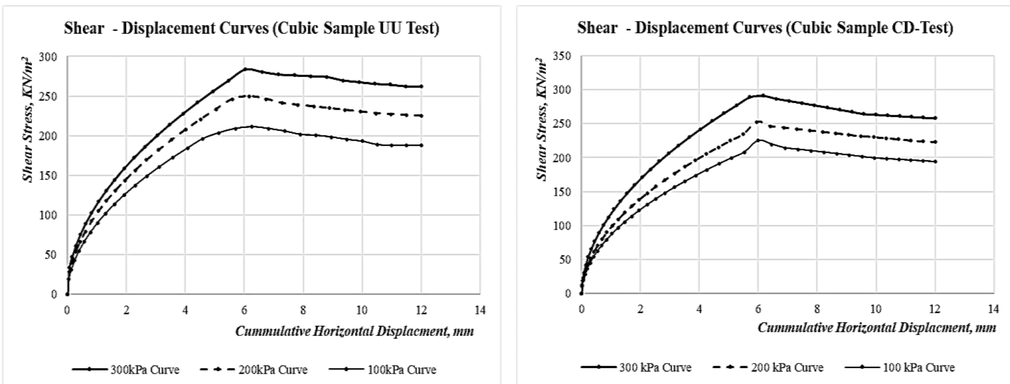


a) b)

**Fig. 9.** Shear Stress vs Displacement Curves for the Cubic Samples:
a) Unconsolidated Undrained (UU) condition; b) Consolidated Drained (CD) condition

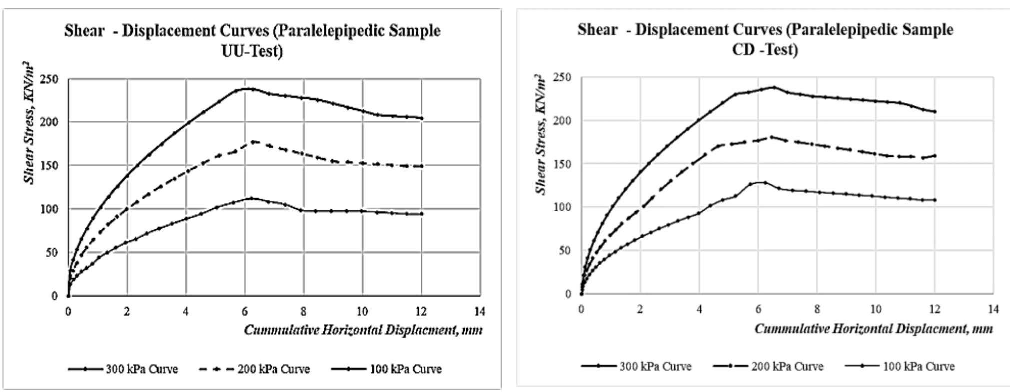


a) b)

**Fig. 10.** Shear stress vs displacement curves for the parallelepipedal samples:

a) Unconsolidated Undrained (UU) condition; b) Consolidated Drained (CD) condition

## Discussions

The results of this study underscore the significance and impact of sample geometry and shearing direction on the shear strength parameters of cohesive soils. The results show that the cubic samples with 6 cm sides and 6 cm height sheared in the vertical direction yielded higher cohesion ($c_2$) values but lower internal friction angles ($\varphi_2$). On the other hand, the parallelepipedic samples, with 2cm height and 6cm sides, sheared horizontally showed higher internal friction angles ($\varphi_1$) but lower cohesion values ($c_1$), thus with approximate differences of ($\varphi_1 = 1.5\ \varphi_2$) $and$ ($c_2 = 2.5c_1$).

The higher cohesion observed in cubic samples can be attributed to the larger volume and shear plane area of the sample which promote a more uniform stress distribution and enhanced interparticle bonding. This suggests that cubic samples might provide a more realistic representation of in-situ conditions in cohesive soils. More so, the cubic configuration helps reduce stress concentrations and edge effects that can lead to premature failure or misleadingly low cohesion values. However, the lower internal friction angles in cubic samples may be due to the increased likelihood of rotational movement within the larger sample, which reduces the effectiveness of particle interlock and frictional resistance.

For the parallelepipedal, the smaller height leads to higher stress concentrations and more pronounced boundary effects, which could increase frictional resistance relative to cohesion. The smaller height limits the potential for rotational movement and hence lead to the increased internal friction angle. This variability in the shear strength parameters is significant for this study as it highlights how the direction of shear and size of sample used in the direct shear test can affect the balance between cohesion and internal friction. This fundamentally brings a new insight into the interpretation of soil shear strength analysis using the direct shear method especially for slope stability analysis.

Slope stability analysis is dependent on accurate soil shear strength parameters, cohesion (c) and the angle of internal friction (ϕ). The higher cohesion values suggest higher resistance to the initiation of the failure surface in cohesive soils and could result in an overall higher resistance to ultimate limit stress (ULS). In slope stability models, incorporating higher cohesion values from cubic samples could lead to a higher estimated factor of safety, particularly in scenarios where soil cohesion is a dominant factor, such as collapsible soils. The higher internal friction angle in the parallelepipedal samples indicate better resistance to shear displacement due to particle interlocking. However, their lower cohesion values could mean that the stability of the slopes may be overestimated if the cohesion is not properly evaluated. For slopes with a high risk of cohesive soil failure (collapsible soils), designs should consider the higher cohesion values while also incorporating safety factors to account for potential lower internal friction angles.

## Conclusions

The analysed dataset obtained from this innovative testing program showed a variability in the shear strength parameters when the direction of shear testing is altered from horizontal to vertical using cubic samples. These differences highlight the variability of soil failure mechanism at the initiation and emergence points on one side, and the point of maximum depth on the other side along the failure surface. This is significant in accurately assessing the shear resistance of soils and their potential failure mechanisms. The differences in shear strength parameters obtained from cubic and parallelepipedal samples bring to light the importance of sample geometry in direct shear testing for interpreting soil behavior. Subsequently, the universal assumption of uniform stress distribution across a soil sample in direct shear testing was observed to be problematic in this study particularly for the parallelepipedal samples where stress concentrations are more likely. Additionally, the fixed horizontal displacement used in for the parallelepipedal samples does not account for strain rate effects which can vary with sample shape and size. The cubic samples used in the new testing program could offer a more reliable indication of in-situ soil behaviour for accurate analysis due to their larger volume and more uniform stress distribution.

For slope stability analysis, the findings of this study postulate a nuanced approach to parameters selection that ensures accurate representation of both cohesion and internal friction in stability models. This approach will lead to more reliable predictions and safer slope designs.

## References

[1] K. Terzaghi, R.B. Peck, *Soil Mechanics in Engineering Practice.* s.l.: John Wiley & Sons, 1948.

[2] O.N. Isaev, R.F Sharafutdinov, *Soil Shear Strength at the Structure Interface.* **Soil Mech Found Eng, Vol. 57**, 2020, p. 139–146.

[3] Y. Yu-qiu, H. Jie, R. Rui., *Assessment of Analytical Solutions for Calculating Lateral Earth Pressures Behind Rigid Retaining Walls Under Translational Movement.* **Geotechnical and Geological Engineering, Vol. 42**, 2024, p. 2901-2919.

[4] B. Tiwari, B. Ajmera, *Advancements in Shear Strength Interpretation, Testing, and Use for Landslide Analysis.*, **Progress in Landslide Research and Technology, Vol. 2**, 2023 p. 3-54.

[5] S.H Jiang, H. Jinsong, Q. Xiao-Hui, Z. Chuang-Bing, *Efficient probabilistic back analysis of spatially varying soil parameters for slope reliability assessment.* **Engineering Geology, Vol. 271**, 2020, p. 105597.

[6] M. Axel, X. Li, F. Wen, M.X An, *Microstructure and Strength Parameters of Cement-Stabilized Loess.* **Geotechnics, Vol. 3**, 2023, p. 161-178.

[7] H. Imran, D. Al-Jeznawi, M.A.Q. Al-Janabi, L.F.A. Bernardo, *Assessment of Soil–Structure Interaction Approaches in Mechanically Stabilized Earth Retaining Walls: A Review.* 3, **CivilEng, Vol. 4**, 2023, p. 982-999.

[8] K. H. Head, R.J. Epps, *Manual of Soil Laboratory Testing, Volume 2: Permeability, Shear Strength and Compressibility Tests.* 3rd. Caithness: Whittles Publishing, 2011.

[9] J. Bai, D. Yu, J. Chenhang, L. Chongyang, Z. Menghan, C. Wang, *A Review of Advances in Triaxial Tests: Instruments, Test Techniques and Prospects.* **KSCE J Civ Eng, Vol. 26**, 2022, p. 3325–3341.

[10] B. James, *Unconfined Compression Test of Soil. [A Descriptive Guide]*. Civil Seek. December 11, 2018.

[11] ASTMD6467, Standard, *Standard Test Method for Torsional Ring Shear Test to Determine Drained Residual Shear Strength of Fine-Grained Soils.* 2021, ASTM International.

[12] D. White, *Geotechnical centrifuge modelling – current practice.* 2020, Physical Models: Their historical and current use in civil and building engineering design.

[13] S.W. Moon, T. Ku, *Empirical estimation of soil unit weight and undrained shear strength from shear wave velocity measurements.* **Australian Geomechanics Society**, 2016, p. 1247-1252.

[14] B.E. Backus, GlobalGilson.com. [Online] n.d. [Cited: June 17, 2024.] https://www.globalgilson.com/blog/soil-direct-shear-test.

[15] N.R. MacDonald, T.R.M. Packulak, J.J. Day, *A Critical Review of Current States of Practice in Direct Shear Testing of Unfilled Rock Fractures Focused on Multi-Stage and Boundary Conditions.* 6, **Geosciences, Vol. 13**, 2023, p. 172.

[16] X. Shiqing, Y. Ben-Zion, J.P. Ampuero, *Properties of inelastic yielding zones generated by in-plane dynamic ruptures—I. Model description and basic results.* **Geophysical Journal International**, 2012, p. 1325–1342.

[17] P. Buck, *Soil Mechanics Vol 1.* 1. Vero Beach: Pile Buck International, Inc., 2023.

[18] A. Stanciu, I. Lungu, *Foundations Vol I - Soil Physics and Mechanics.* Bucharest: Technical Publishing House, 2006.

[19] A. Stanciu, I.C. Herta, C. Predoaie, *Device for direct shear along on imposed vertical plan of soil samples.* **134239 Romania**, 2020.

[20] L. Zhu, Q. Liao, Z. Wang, J. Chen, Z. Chen, Q. Bian, Q. Zhang, *Prediction of Soil Shear Strength Parameters Using Combined Data and Different Machine Learning Models.* 10, **Applied Sciences, Vol. 12**, 2022, p. 5100.

*Received: May 10, 2024*
*Accepted: June 16, 2024*